Optical absorption in molecular crystals from time-dependent density functional theory

Leeor Kronik
WEIZMANN INSTITUTE OF SCIENCE

04/18/2017
Final Report

FORM SF 298

REPORT DOCUMENTATION PAGE

Form Approved
OMB No. 0704-0188

1. REPORT DATE *(DD-MM-YYYY)*	2. REPORT TYPE	3. DATES COVERED *(From - To)*
23-04-2017	Final	01 Sep 2015 to 31 Aug 2016

4. TITLE AND SUBTITLE
Optical absorption in molecular crystals from time-dependent density functional theory

5a. CONTRACT NUMBER

5b. GRANT NUMBER
FA9550-15-1-0290

5c. PROGRAM ELEMENT NUMBER
61102F

6. AUTHOR(S)
Leeor Kronik

5d. PROJECT NUMBER

5e. TASK NUMBER

5f. WORK UNIT NUMBER

7. PERFORMING ORGANIZATION NAME(S) AND ADDRESS(ES)
WEIZMANN INSTITUTE OF SCIENCE
200 Herzl
Rehovot, 000076270 IL

8. PERFORMING ORGANIZATION REPORT NUMBER

9. SPONSORING/MONITORING AGENCY NAME(S) AND ADDRESS(ES)
EOARD
Unit 4515
APO AE 09421-4515

10. SPONSOR/MONITOR'S ACRONYM(S)
AFRL/AFOSR IOE

11. SPONSOR/MONITOR'S REPORT NUMBER(S)
AFRL-AFOSR-UK-TR-2017-0030

12. DISTRIBUTION/AVAILABILITY STATEMENT
A DISTRIBUTION UNLIMITED: PB Public Release

13. SUPPLEMENTARY NOTES

14. ABSTRACT
We address a major challenge for computational materials science based on density functional theory, by showing that fundamental gaps and optical spectra of molecular solids can be predicted quantitatively and non-empirically within the framework of time-dependent density functional theory (TDDFT), using the recently-developed optimally-tuned screened range-separated hybrid (OTSRSH) approach. We provide a comprehensive benchmark for the accuracy of our approach by considering the X23 set of molecular solids and comparing results obtained from TDDFT with those obtained from many-body perturbation theory in the GW-BSE approximation. We additionally compare results obtained from dielectric screening computed within the random phase approximation to those obtained from the computationally easier many-body dispersion approach and find that this influences the fundamental gap but there is little effect on the optical spectra. We therefore believe that the method is robust and can be used for studies of molecular solids that are typically outside the reach of computationally more intensive methods.

15. SUBJECT TERMS
EOARD, Materials, optical absorption, dft

16. SECURITY CLASSIFICATION OF:			17. LIMITATION OF ABSTRACT	18. NUMBER OF PAGES	19a. NAME OF RESPONSIBLE PERSON
a. REPORT	b. ABSTRACT	c. THIS PAGE	SAR	13	FOLEY, JASON
Unclassified	Unclassified	Unclassified			**19b. TELEPHONE NUMBER** *(Include area code)* 011-44-1895-616036

Standard Form 298 (Rev. 8/98)
Prescribed by ANSI Std. Z39.18

Optical absorption in molecular crystals from time-dependent density functional theory

Final report for the European Office of Aerospace Research & Development Grant No. FA9550-15-1-0290

Leeor Kronik[1]

[1]*Department of Materials and Interfaces, Weizmann Institute of Science, Rehovoth 76100, Israel*

We address a major challenge for computational materials science based on density functional theory, by showing that fundamental gaps and optical spectra of molecular solids can be predicted quantitatively and non-empirically within the framework of time-dependent density functional theory (TDDFT), using the recently-developed optimally-tuned screened range-separated hybrid (OT-SRSH) approach. In this scheme, the electronic structure of the gas-phase molecule is determined by optimal tuning of the range-separation parameter in a range-separated hybrid functional. Screening and polarization in the solid-state are taken into account by adding long-range dielectric screening to the functional form, with the modified functional used to perform self-consistent periodic-boundary calculations for the crystalline solid. We provide a comprehensive benchmark for the accuracy of our approach by considering the X23 set of molecular solids and comparing results obtained from TDDFT with those obtained from many-body perturbation theory in the GW-BSE approximation. We additionally compare results obtained from dielectric screening computed within the random-phase approximation to those obtained from the computationally easier many-body dispersion approach and find that this influences the fundamental gap but there is little effect on the optical spectra. We therefore believe that the method is robust and can be used for studies of molecular solids that are typically outside the reach of computationally more intensive methods. The work is now being written up for publication.

I. INTRODUCTION

The electronic and optical properties of molecular solids have recently attracted significant attention, primarily in the context of optoelectronic devices based on small molecules (see, e.g., Refs. 1–4). In particular, there is on-going interest in identifying small-gap organic molecules for high-performance, low-cost, or enhanced-stability optoelectronic devices based on solids synthesized from these molecules (see, e.g., Refs. 5–9, for some recent overviews). Theory can and should play an important role in such investigations, as it can clarify the properties of existing molecular solids and point out promising new ones [10–13].

Electronic properties, such as the band structure in general and the transport gap in particular, and optical properties, such as optical absorption in general and the optical gap in particular, are excited-state properties. For inorganic solids, these properties have long been calculated using many-body perturbation theory (MBPT).[14–16] In MBPT, Dyson's equation is often solved using Hedin's GW approximation,[17] where G is the one-particle Green function and W is the dynamically screened Coulomb interaction.[14, 18] The Bethe-Salpeter equation (BSE) for the two-particle Green function is then solved approximately to predict optical properties.[14, 19, 20] In recent years, the GW-BSE approach has been increasingly applied to molecular solids, yielding many important insights (see Ref. 13 for a recent overview). Unfortunately, such GW-BSE calculations can be quite expensive and complicated, limiting

our ability to use them routinely, especially in the context of high-throughput calculations for new materials.

Density functional theory (DFT), in both its time-independent [21, 22] and time-dependent [23–26] forms, suitable for ground and excited state properties, respectively, is much more efficient computationally. However, common approximations to time-dependent DFT (TDDFT) are known to fail in the solid-state limit [14, 27]. For molecular solids in particular, key quantities, such as the transport gap, the optical gap, and the exciton binding energy (i.e., the difference between the two gaps), are often in qualitative or gross quantitative error.[13]

Recently, Refaely-Abramson *et al.* have suggested the optimally-tuned screened range-separated hybrid (OT-SRSH) functional as a means for quantitative DFT-based prediction of excited-state properties in molecular solids.[28, 29] In this approach, one first computes the underlying gas-phase molecule using an asymptotically correct range-separated hybrid (RSH) functional, in which an optimal range-separation parameter is determined non-empirically,[30–33] based on satisfaction of the ionization potential theorem. One then uses the same range-separation parameter in the solid-state environment, while accounting explicitly for solid-state polarization by screening the asymptotic potential with a non-empirical dielectric constant.[28, 29]

While preliminary results obtained with the OT-SRSH method have shown excellent agreement with GW-BSE data, two important questions remain. First, results have been reported to-date only for only two molecular solids -

pentacene[28, 29] and quinacridone,[34] an air-stable pentacene derivative, with the optical absorption spectrum spectra computed only for the former. The validity of the OT-SRSH approach across a wider range of molecular crystals is therefore in need of demonstration. Second, previous OT-SRSH calculations have used the dielectric constant obtained within the random-phase approximation (RPA) for facilitating comparison to MBPT data. However, this step can itself be expensive and it remains to be seen whether sufficiently accurate results can be obtained from more simple methods for determining the dielectric constant.

In this article, we address both questions by assessing the accuracy of the OT-SRSH approach for transport gaps and optical absorption spectra across the X23 set of molecular solids.[35, 36] This set comprises crystals based on small- to medium-sized organic molecules, possessing a variety of weak inter-molecular interactions and different degrees of solid-state polarization. It therefore provides a strict benchmark for OT-SRSH capabilities. We further compare results obtained using an RPA-based dielectric constant with those obtained using many-body dispersion (MBD). Within the RPA, we find our OT-SRSH results to be in very good agreement with those obtained from GW for quasi-particle gaps and from GW-BSE for the optical spectrum. We further find that using MBD-based dielectric screening results in larger deviations for quasi-particle gaps but has an essentially negligible effect on the optical absorption, allowing for an inexpensive yet non-empirical prediction of optical properties.

II. THEORETICAL AND COMPUTATIONAL APPROACH

A. Optimally-tuned range-separated hybrid functionals

In the range-separated hybrid (RSH) method, the Coulomb interaction is range-split. Here, we use the range-separation scheme suggested by Yanai *et al.*,[37] which is based on the identity:

$$\frac{1}{r} = \frac{\alpha + \beta \mathrm{erf}(\gamma r)}{r} + \frac{1 - [\alpha + \beta \mathrm{erf}(\gamma r)]}{r}. \quad (1)$$

where r is the inter-electron coordinate and α, β, γ are parameters. The full $1/r$ repulsion is used for the Hartree and correlation terms, but the two terms on the right-hand side of Eq. (1) are treated differently in the computation of the exchange term. The first term is treated using exact (i.e., Fock) exchange, whereas the second term is treated using local or semi-local exchange. This leads to the following expression for the exchange-correlation energy, E_{xc}:

$$E_{xc}^{RSH} = \alpha E_{xx}^{SR} + (1 - \alpha) E_{DFAx}^{SR} + (\alpha + \beta) E_{xx}^{LR}$$
$$+ (1 - \alpha - \beta) E_{DFAx}^{LR} + E_{DFAc}, \quad (2)$$

where the super-scripts 'SR' and 'LR' denote short-range and long-range contributions, respectively, and the subscripts 'xx', 'DFAx' and 'DFAc' denote Fock-like exact exchange, approximate (semi-)local exchange, and approximate (semi-)local correlation, respectively.[38] Equation (2) reveals that the parameter α dictates the amount of Fock-like exchange in the short range ($r \to 0$) and the parameter sum $\alpha + \beta$ determines the amount of Fock-like exchange in the long range ($r \to \infty$). The two limits are smoothly interpolated using the error function, with γ being the range-separation parameter, i.e., $1/\gamma$ corresponds to a typical length denoting the transition from SR to LR.

In order to turn Eq. (2) into a practical functional, one needs to choose the approximate (semi-)local exchange-correlation functional and set the parameters α, β, and γ. To proceed without introducing empiricism, typical choices for the (semi-)local functional would be the local density approximation, LDA,[39] or the Perdew-Burke-Ernzerhof (PBE)[40] form of the generalized-gradient approximation (GGA). In some cases, the fraction of SR Fock exchange, α, can be determined from first-principles based on satisfaction of piecewise linearity in fractional DFT [38, 41], but this is not always possible.[42] For a wide variety of organic molecules a universal value of 0.2 has been found to be useful (see, e.g., Refs. 28, 38, 41–43). This value is used in this work throughout. For any choice of α, the condition $\alpha + \beta = 1$ guarantees 100% of LR Fock exchange and therefore the correct asymptotic potential in the gas phase.[30, 38, 41]

In many popular RSH functionals, the range-separation parameter, γ, is given a universal value based on fitting against an appropriate data set.[31, 37, 43–45] In the optimal tuning (OT) scheme, γ is system-dependent, but still chosen non-empirically. For gas-phase systems, it is obtained by satisfying the ionization potential (IP) theorem,[46–49] which states that for the exact functional the energy of the highest occupied molecular orbital (HOMO) is equal and opposite to the ionization potential, i.e., $IP = -\epsilon_{HOMO}$. Often, this condition is demanded simultaneously for the system in both its neutral and anionic state (where the ionization potential corresponds to the electron affinity of the neutral). [30, 31, 50] For any choice of α, the optimal tuning scheme then involves the minimization of a target function, $J(\gamma; \alpha)$, defined by:

$$J^2(\gamma; \alpha) = \sum_{i=N, N+1} [IP^{\gamma;\alpha}(i) + \varepsilon_H^{\gamma;\alpha}(i)]^2. \quad (3)$$

Minimizing this target function has been shown to be equivalent to enforcing piecewise linearity [33, 34, 41, 51–53], resulting in an accurate prediction of the ionization potential and the electron affinity directly from the energy levels of the highest occupied and lowest unoccupied orbitals, respectively.[31, 33, 54]

Refaely-Abramson *et al.* have suggested that the OT-RSH scheme can be extended to molecular solids by using a *screened* range-separated hybrid (SRSH).[28] Briefly, in

this approach one first selects α and γ for the gas-phase molecule as described above. One then notes that in the gas-phase the asymptotic potential is $-1/r$ but in the solid state it is $-1/(\epsilon r)$, where ϵ is the scalar dielectric constant. Therefore β is re-adjusted to reflect this screening, by demanding that $\alpha+\beta = 1/\epsilon$ instead of $\alpha+\beta = 1$ as in the gas-phase. The resulting *screened* RSH functional is then applied to the molecular solid.[13, 28, 29, 34]

B. The X23 set of molecular solids

For evaluating the accuracy of the above approach in a systematic manner, we consider quasi-particle (QP) gaps and optical absorption spectra for the set of 23 non-covalently bound molecular solids, known as the X23 set.[35] A schematic diagram displaying all molecular entities considered in this set is given in Figure 1. The molecules used are small- to medium-sized organic molecules that can be grouped into four subsets based on their chemical identity: Open-cyclic aliphatic molecules (carbon dioxide, ammonia, acetic acid, succinic acid, cyanamide, ethyl carbamate, oxalic acid (in both α and β polymorphs), urea, and formamide), cyclic aliphatic molecules (adamantane, hexamine, trioxane, and 1,4-cyclohexane-di-one), cyclic aromatic molecules (benzene, naphthalene, and anthracene), and heterocyclic aromatic molecules (cytosine, uracil, triazine, imidazole, pyrazine, and pyrazole). In crystalline solid form, these molecules are weakly bound, typically through H-bonding, $\pi-\pi$ stacking, van der Waals interactions, etc.
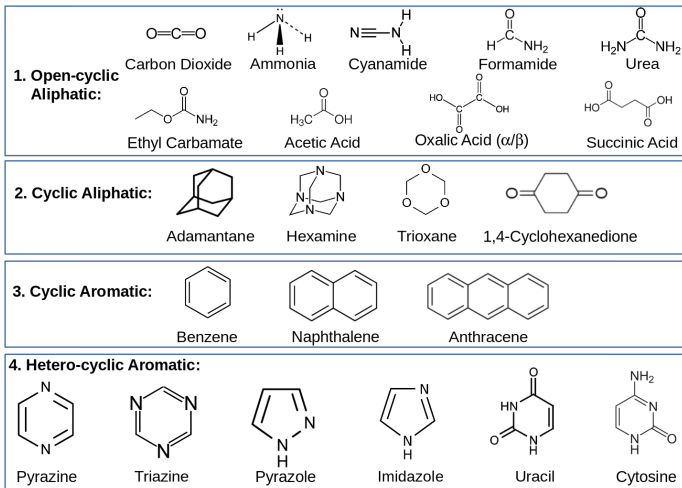

FIG. 1: (Color online) Chemical structures of all organic molecules present in the X23 molecular crystal set.

C. Computational Details

All gas-phase OT-RSH calculations presented in this work were based on the LRC-ωPBE0 RSH functional,[43], which is based on Eq. 2 with $\alpha=0.2$ and PBE correlation and short-range exchange components, as implemented in the Q-CHEM code (version 4.3) [55], but with the range-separated parameter γ optimally-tuned per system, rather than fixed to its default value. Optimization proceeded via minimization of the target function J given in Eq. (3), i.e., both neutral and anion were considered, except for molecules exhibiting an unbound LUMO, where only the neutral form was considered. The all-electron cc-pVTZ basis set was used throughout for all atoms.

All solid-state OT-SRSH calculations were carried out using PARATEC (revision 499),[56] modified a pseudopotential-planewave code. Here, short-range LDA exchange was used, together with LDA correlation, again with $\alpha=0.2$ throughout. Differences in tuning based on LDA or PBE were found to be insignificant. See Refs. 28, 29 for more implementation details. LDA-based Troullier-Martins [57] norm-conserving pseudopotentials, adapted from the ABINIT website,[58] were used for all atoms. An energy cutoff of 816 eV was used throughout. Two different methods were used to evaluate the scalar dielectric constant needed for the determination of β in the solid-state calculations. In one, we used the random phase approximation (RPA), as used in the G_0W_0 calculations elaborated below. In the other, we used the many-body dispersion (MBD) approach.[59]

For comparison purposes, all molecular solids were also computed using a standard one-shot perturbative G_0W_0 calculation,[13, 18] based on the DFT eigenvalues and eigenvectors obtained from am LDA calculation within PARATEC. We used a generalized plasmon pole model [18], implemented within the BerkeleyGW package (trunk version, revision 6539).[60] This approach has previously been established as a quantitatively useful tool for the study of molecular solids (see Ref. 13, and references therein).

Optical spectra in the solid state were computed using TDDFT with the LDA and the OT-SRSH functional, as well as with the Bethe-Salpeter equation (BSE) based on the G_0W_0 output. Both TDDFT and BSE calculations were performed using the BerkeleyGW package [60], modified to include TDDFT, with incident light polarization averaged over the main unit-cell axes. The kernel was calculated on a coarse wavefunction grid, then interpolated to a fine grid using the interpolation scheme suggested by Rohlfing and Louie. [61] We used a slightly shifted grid to generate the transition matrix elements in the dielectric function, using a velocity operator to approximate an incident light along a specific direction. [61] Grid shift directions were set along the a, b, and c unit-cell axes. For large crystals, we only used one grid in the TDDFT calculations as they are easier to converge with respect to k-point sampling.

III.   RESULTS AND DISCUSSION

A.   Fundamental gap

We begin our benchmark evaluation by comparing the fundamental gaps computed using OT-SRSH and G_0W_0 methods for all solids in the X23 set. To prevent clouding the comparison by a different treatment of the dielectric constant, all OT-SRSH results presented are based on the dielectric constant obtained within RPA, except in the last part of this section, where comparison with MBD-based results is explicitly made. With both OT-SRSH and GW, we computed the fundamental gap as the energy difference between the highest occupied and lowest unoccupied state at the Γ point of the Brillouin zone, as the inter-molecular orbital hybridization and therefore band dispersion are very small.

All computed fundamental gaps are given in Table I, where they are additionally compared to LDA-computed gaps. It is readily observed that the OT-SRSH gaps agree very well indeed with the GW ones. The deviation between the gaps computed with both methods is summarized graphically in Fig. 2. The differences are usually 0.2 eV at most, with a mean absolute deviation of only 0.15 eV. Only two solids (hexamine and imidazole) exhibited a somewhat larger deviation of 0.3 eV and only one solid (pyrazole) exhibits a larger deviation of 0.5 eV. Not surprisingly, these gaps are substantially larger than those obtained with LDA, which is well-known to underestimate fundamental gaps in general.[14, 18] A comparison of the solid-state, OT-SRSH-computed fundamental gaps with the gas-phase, OT-RSH computed ones (not shown for brevity) reveals that, as expected, the gas-phase gaps are substantially larger than the solid-state ones (by as little as 0.8 eV and as much as 4.8 eV). This reflects the well-known phenomena of polarization-induced gap-renormalization in molecular solids,[62] which is clearly captured in the OT-SRSH scheme [28] but is known to be absent in standard functionals [13, 63].

The above results establish dielectric screening as key to accurate treatment of molecular solids. Indeed, there is growing recent interest in solid-state screening as an ingredient in the construction of density functionals in general (see, e.g., [29, 64–68]). We also note that specifically for molecular solids, there is growing interest in embedding a range-separated hybrid molecular calculation within a polarizable continuum model to mimic solid-state effects (see, e.g., [69, 70]). Our approach represents a full solid-state calculation, allowing for polarization effects while still capable of capturing inter-molecular dispersion effects [28].

B.   Optical Absorption Spectra

We next compare the optical absorption spectra calculated using TD-OT-SRSH with those obtained from the G_0W_0-BSE methods. As we are interested in allowed

TABLE I: Fundamental gaps of the X23 set of molecular solids (in eV), calculated using LDA, OT-SRSH and G_0W_0.

| Molecular Solid	Fundamental Gap (E_g)		
	LDA	OT-SRSH	G_0W_0
Carbon dioxide	6.4	11.2	11.2
Ammonia	4.3	7.9	7.7
Cyanamide	4.6	8.0	8.0
Formamide	4.9	8.8	8.8
Urea	4.8	8.0	7.9
Ethyl carbamate	5.6	9.0	8.8
Acetic acid	5.1	9.1	9.3
Oxalic acid (α)	3.2	6.7	6.9
Oxalic acid (β)	3.5	7.3	7.5
Succinic acid	5.2	9.1	9.1
Adamantane	4.8	7.5	7.6
Hexamine	5.0	7.5	7.8
Trioxane	5.9	9.7	9.5
1,4-Cyclohexane-di-one	3.5	7.0	7.0
Benzene	4.3	6.8	6.9
Naphthalene	3.2	5.2	5.4
Anthracene	2.1	3.9	4.1
Pyrazine	2.8	6.2	6.0
Triazine	3.0	6.2	6.3
Pyrazole	4.8	7.6	8.1
Imidazole	4.8	7.6	7.9
Uracil	3.4	6.4	6.4
Cytosine	3.4	6.1	6.1
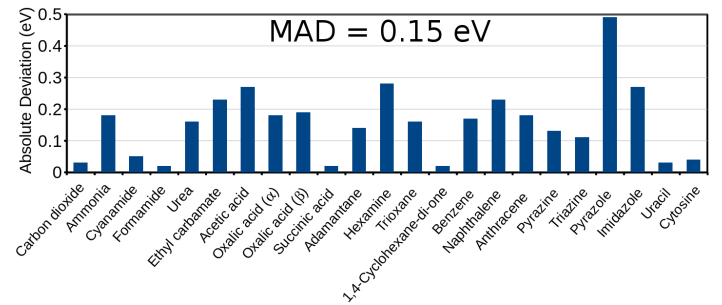
FIG. 2: (Color online) Absolute deviations and mean absolute deviation (MAD) in the calculated quasi-particle gap between the OT-SRSH and G_0W_0 for the X23 set of molecular solids. For OT-SRSH calculations, the G_0W_0 computed RPA macroscopic dielectric constant (ϵ^{RPA}) is used.

optical transitions, we only consider singlet excitations. The complete set of optical absorption spectra is shown in Figs. 3 and 4, for solids based on aliphatic and aromatic molecules, respectively. In addition, the energy of the lowest singlet excitation and the position of lowest-lying main optical absorption peak (i.e., the lowest singlet excitation with non-negligible oscillator strength) are provided in Table II, along with experimental values for comparison, where available.

It is readily observed from Figs. 3 and 4 that absorption spectra computed with the TD-OT-SRSH approach do indeed agree well with those computed using G_0W_0-BSE, across the board, over a range of several eV. Specifically, the position of intense peaks, found by the two approaches, typically agrees within ~0.2-0.3 eV, which is as good as can possibly be expected given an accuracy of
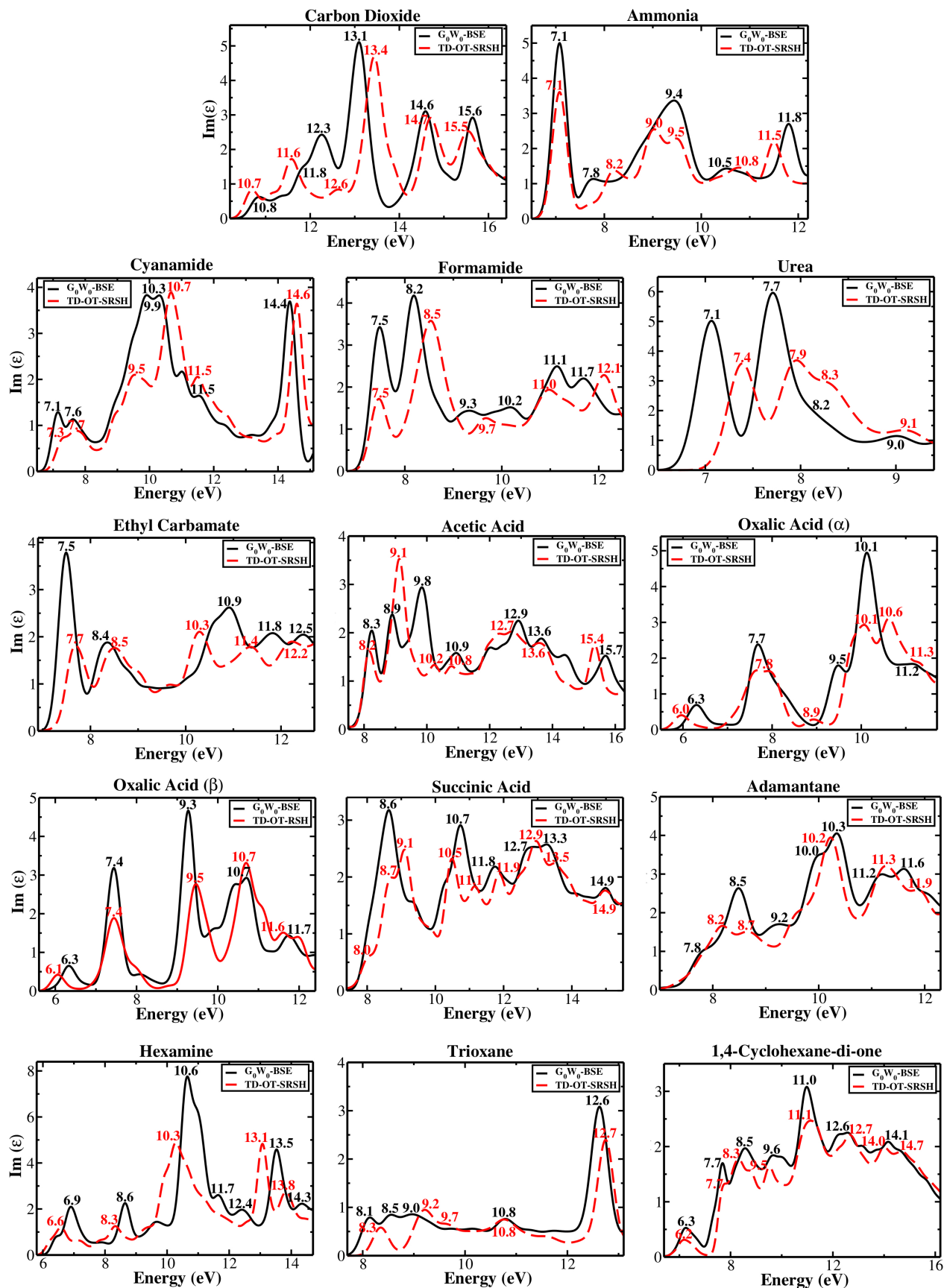
FIG. 3: (Color online) The imaginary part of the dielectric function of aliphatic-molecule-based solids in the X23 data set, calculated using G_0W_0/BSE (black, solid lines) and TD-OT-SRSH (red, dashed lines).
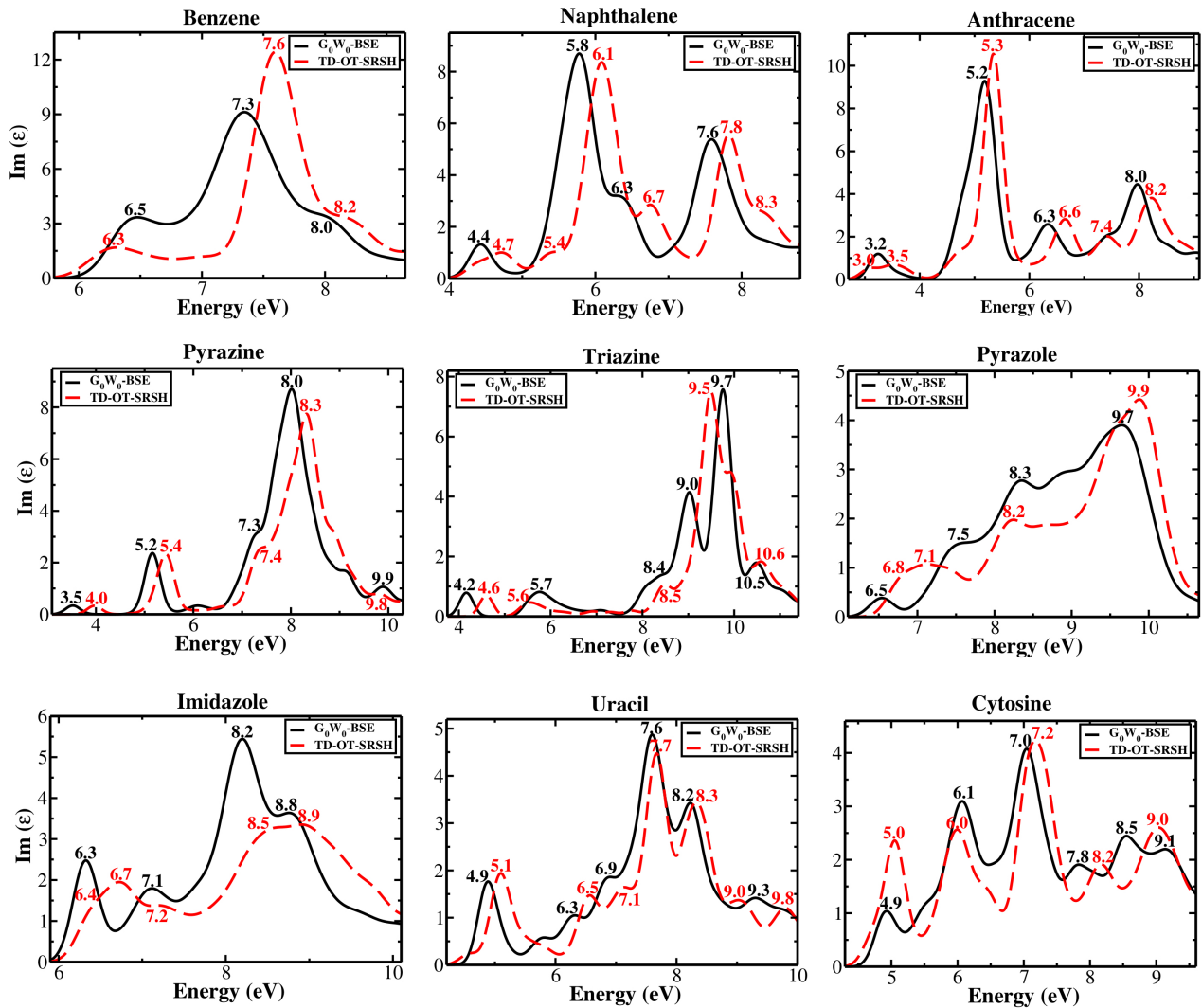
FIG. 4: (Color online) The imaginary part of the dielectric function of aromatic-molecule-based solids molecules in the X23 data set, calculated using G_0W_0/BSE (black, solid lines) and TD-OT-SRSH (red, dashed lines).

~0.1 eV at best for either approach separately. This observation is quantified in Fig. 5, which shows deviations between peak positions using TD-OT-SRSH and GW-BSE, for the lowest-energy peak (top) and for all peaks shown in Figs. 3 and 4 (bottom). Clearly, the mean absolute deviation is only 0.2 eV for either the lowest-energy peak or all shown peaks, with deviations rarely exceeding 0.3 eV.

As expected based on known shortcomings of TDLDA [13, 14, 27], the TD-OT-SRSH data offer an improvement over TDLDA data that is not only quantitative but also qualitative. This is demonstrated in Fig. 6 for two representative cases - the ammonia and uracil solids. For ammonia, TDLDA produces an extended spurious absorption "tail", starting at ~4.5 eV, whereas both TD-OT-SRSH and GW-BSE predict a sharp onset of absorption, at ~7.0 eV. The same phenomenon has been previously observed for a non-molecular solid - LiF [29]. For uracil,

TDLDA produces a spurious peak at ~3.8 eV. Further analysis (not shown for brevity) reveals that this peak results from LDA mis-ordering of the HOMO and HOMO-1 orbitals, which is remedied by the OT-SRSH calculation and removes the false peak.

In many of the molecular solids, the lowest singlet excitation possesses a small matrix element and contributes little to the optical spectrum. This is reflected in Table II, where the energy of the first-excited state is often predicted to be quite different from the energy of the lowest-lying absorption peak, using either TD-OT-SRSH or GW-BSE. We found that larger differences between the two methods often, but not always, arise for these low-absorption excitations, despite the excellent agreement in predictions of the fundamental gap and the high-absorption excitations. As an example, for ammonia the lowest-energy singlet excitation is predicted to be 6.7 or 6.6 eV using TD-OT-SRSH or GW-BSE, respectively,
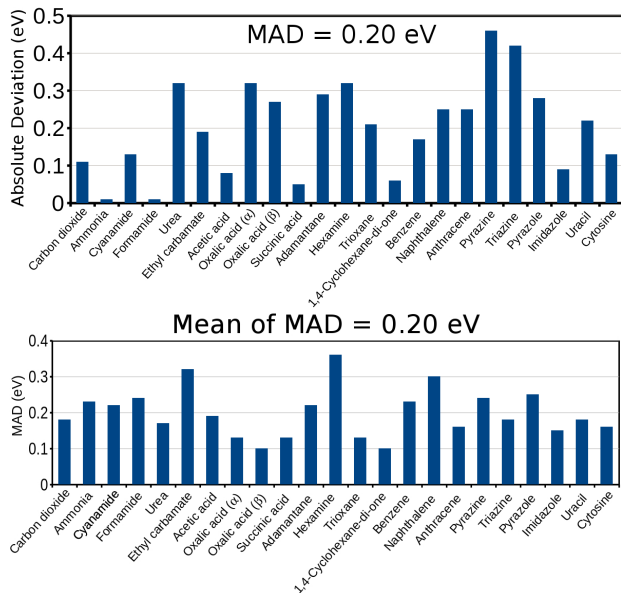
FIG. 5: (Color online) Absolute deviations between the TD-OT-SRSH and G_0W_0-BSE computed peak positions in the optical spectra of the X23 molecular solid set. Top: lowest peak position. Bottom: Mean absolute deviations of all peaks shown in Fig. 3 or 4.

with both values in excellent agreement with the experimental values of 6.6 eV. [72] A similar picture emerges for adamantane. But for urea or 1,4-cyclohexane-di-one, the difference between the two predictions is a much larger and entirely non-negligible 0.6 eV. We note that these lowest-lying transitions often involve transitions between highly localized orbitals, which can exhibit large self-interaction errors. Therefore the discrepancy may be due to remaining issues in the TDDFT calculation, but may well be also due to LDA being an insufficient starting point for the GW-BSE calculation.[82–84] We note that such issues are not necessarily related to strongly localized states, as both GW starting point and remaining TD-OT-SRSH inaccuracies have also been pointed for benzene and oligoacene molecules and solids [29, 42, 84–86]. As this barely affects the optical spectrum, the matter is not pursued further here.

C. Effect of the dielectric constant

To facilitate comparison to GW-BSE, which relies on evaluation of the dielectric function using the random-phase approximation (RPA), all OT-SRSH and TD-OT-SRSH results reported above were obtained using ϵ^{RPA}. Here, we explore the effect of basing the calculation on an evaluation of the dielectric constant using the inexpensive many-body dispersion (MBD) method [59]. A comparison of dielectric constants and quasi-particle gaps obtained from using ϵ^{RPA} and ϵ^{MBD} (not shown for

brevity) reveals that $\epsilon^{MBD} \geq \epsilon^{RPA}$ throughout the X23 set, likely because it is computed based on PBE, which tends to overestimate polarizabilities. Therefore, the MBD-computed fundamental gaps are generally smaller than RPA-computed ones. While the difference is often small, it can be substantial - as much as 0.8 eV for succinic acid and 0.7 eV for uracil. It would be interesting to examine whether an iteration of the ϵ value, from MBD calculations based on the OT-SRSH calculation, would result in improved agreement.

While the differences in the dielectric constant do affect the fundamental gap, their effect on the optical spectra is much smaller. This is reasonable, as the fundamental gap reflects charged excitations, whereas optical excitations are neutral. The effect of the dielectric constant on the TD-OT-SRSH absorption spectra is demonstrated in Figure 7, for the case of the acene-based molecular solids. Clearly, the effect of ϵ is marginal (e.g., differences of ∼0.1 eV at most in the absorption peak position for the benzene solid). The effect on the lowest singlet-excitation energy is equally small. Therefore, using MBD dielectric constants leads to an inexpensive and predictive calculation of optical spectra in molecular solids.

IV. CONCLUSIONS

In conclusion, we have computed fundamental gaps and optical spectra for the entire X23 benchmark set of molecular solids using the recently developed optimally-tuned screened range-separated hybrid functional approach. In this two-stage approach, optimal tuning of a range-separated hybrid functional is first used for an accurate and predictive calculation of the gas-phase electronic structure. Dielectric screening is then built into the functional to obtain a self-consistent prediction for the solid-state electronic structure and optical properties. The obtained results have been compared to many-body perturbation theory calculations within the GW-BSE approach. Agreement has been found to be very good to excellent throughout, with somewhat larger differences possible for optically dark singlet excitations that do not affect the optical spectrum. Furthermore, we have shown that inexpensive evaluation of the dielectric constant using many-body dispersion is sufficient for obtaining accurate optical spectra, opening the door to low-cost, fully predictive calculation of optical spectra in molecular solids.
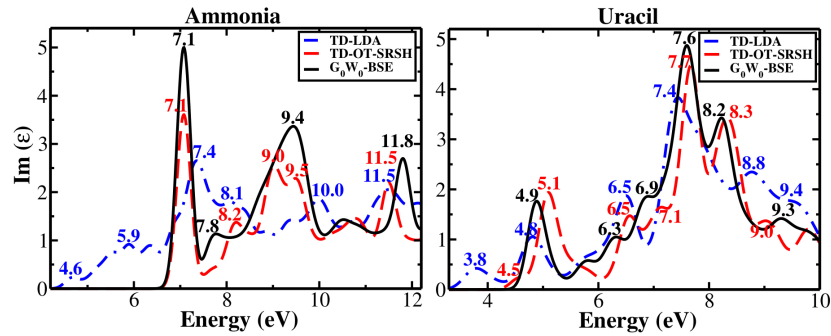
FIG. 6: (Color online) The imaginary part of the dielectric function of the ammonia and uracil molecular solids, calculated using G_0W_0/BSE (black, solid lines), TD-OT-SRSH (red, dashed lines), and TDLDA (dotted, blue lines).
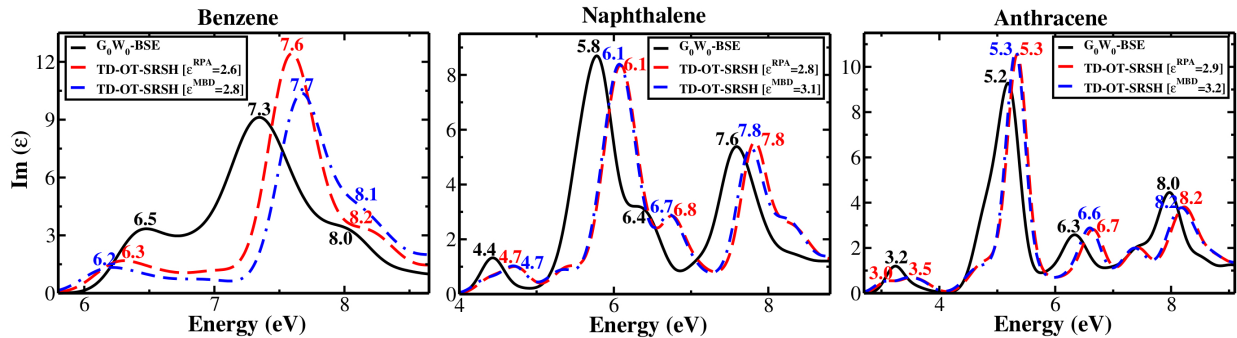

FIG. 7: (Color online) The imaginary part of the dielectric function for the aromatic acene molecular solids (benzene, naphthalene and anthracene), calculated using G_0W_0/BSE (black, solid lines), TD-OT-SRSH based on ϵ^{RPA} (red, dashed lines)], and TD-OT-SRSH based on ϵ^{MBD} (blue, dash-dotted lines). The different ϵ values are denoted in the figure.

[1] S. R. Forrest and M. E. Thompson, Chem. Rev. **107**, 923 (2007).

[2] N. Kaur, M. Singh, D. Pathak, T. Wagner, and J. Nunzi, Synthetic. Metals **190**, 20 (2014).

[3] K.-J. Baeg, M. Binda, D. Natali, M. Caironi, and Y.-Y. Noh, Adv. Mater. **25**, 4267 (2013).

[4] W. Hu, F. Bai, X. Gong, X. Zhan, H. Fu, and T. Bjornholm, *Organic Optoelectronics, 1st Edition* (Wiley-VCH, Heidelberg, 2013).

[5] X.-C. Li, C.-Y. Wang, W.-Y. Lai, and W. Huang, J. Mater. Chem. C **4**, 10574 (2016).

[6] J.-X. Dong and H.-L. Zhang, Chinese Chem. Lett. **27**, 1097 (2016).

[7] T. C. Parker, D. G. D. Patel, K. Moudgil, S. Barlow, C. Risko, J.-L. Brédas, J. R. Reynolds, and S. R. Marder, Mater. Horiz. **2**, 22 (2015).

[8] D. Li, H. Zhang, and Y. Wang, Chem. Soc. Rev. **42**, 8416 (2013).

[9] B. Lucas, T. Trigaud, and C. Videlot-Ackermann, Polymer International **61**, 374 (2012).

[10] J.-L. Brédas, J. E. Norton, J. Cornil, and V. Coropceanu, Acc. Chem. Res. **42**, 1691 (2009).

[11] B. M. Savoie, N. E. Jackson, T. J. Marks, and M. A. Ratner, Phys. Chem. Chem. Phys. **15**, 4538 (2013).

[12] C. Risko and J.-L. Brédas, *Small Optical Gap Molecules and Polymers: Using Theory to Design More Efficient*

Materials for Organic Photovoltaics (Springer, Berlin, 2014), pp. 1–38, ISBN 978-3-662-43874-9.

[13] L. Kronik and J. B. Neaton, Annu. Rev. Phys. Chem. **67**, 587 (2016).

[14] G. Onida, L. Reining, and A. Rubio, Rev. Mod. Phys., **74** (2002).

[15] G. Strinati, Riv. Nuovo Cimento **11**, 1 (1988).

[16] W. G. Aulbur, L. Jonsson, and J. W. Wilkins, Solid State Phys. **54**, 1218 (2000).

[17] L. Hedin, Phys. Rev. **139** (1965).

[18] M. Hybertsen and M. Louie, Phys. Rev. B **34** (1986).

[19] M. Rohlfing and S. G. Louie, Phys. Rev. Lett. **81**, 2312 (1998).

[20] S. Albrecht, L. Reining, R. Del Sole, and G. Onida, Phys. Rev. Lett. **80**, 4510 (1998).

[21] E. K. U. Gross and R. M. Dreizler, *Density Functional Theory* (Plenum, New York, 1995).

[22] R. G. Parr and W. Yang, *Density Functional Theory of Atoms and Molecules* (Oxford University Press, Oxford, 1989).

[23] M. A. Marques, N. T. Maitra, F. M. Nogueira, E. K. U. Gross, and A. Rubio, *Fundamentals of Time-Dependent Functional Theory*, vol. 837 (Springer, Berlin, 2012).

[24] M. E. Casida, *in Recent Advances in Density-Functional Methods part I* (World Scientific, Singapore, 1995).

[25] K. Burke, J. Werschnik, and E. K. U. Gross, J. Chem.

Phys. **123**, 062206 (2005).

[26] C. A. Ullrich, *Time-Dependent Density-Functional Theory: Concepts and Applications* (Oxford University Press, Oxford, 2012).

[27] N. T. Maitra, J. Chem. Phys. **144**, 220901 (2016).

[28] S. Refaely-Abramson, S. Sharifzadeh, M. Jain, R. Baer, J. B. Neaton, and L. Kronik, Phys. Rev. B **88**, 081204 (2013).

[29] S. Refaely-Abramson, M. Jain, S. Sharifzadeh, J. B. Neaton, and L. Kronik, Phys. Rev. B **92**, 081204 (2015).

[30] T. Stein, L. Kronik, and R. Baer, J. Am. Chem. Soc. **131**, 2818 (2009).

[31] T. Stein, H. Eisenberg, L. Kronik, and R. Baer, Phys. Rev. Lett. **105**, 266802 (2010).

[32] S. Refaely-Abramson, R. Baer, and L. Kronik, Phys. Rev. B **84**, 075144 (2011).

[33] L. Kronik, T. Stein, S. Refaely-Abramson, and R. Baer, J. Chem. Theo. Comput. **8**, 1515 (2012).

[34] D. Lüftner, S. Refaely-Abramson, M. Pachler, R. Resel, M. G. Ramsey, L. Kronik, and P. Puschnig, Phys. Rev. B **90**, 075204 (2014).

[35] A. M. Reilly and A. Tkatchenko, J. Chem. Phys. **139**, 024705 (2013).

[36] A. Otero-de-la Roza and E. R. Johnson, J. Chem. Phys. **137**, 054103 (2012).

[37] T. Yanai, D. P. Tew, and N. C. Handy, Chem. Phys. Lett. **393**, 51 (2004).

[38] S. Refaely-Abramson, S. Sharifzadeh, N. Govind, J. Autschbach, J. B. Neaton, R. Baer, and L. Kronik, Phys. Rev. Lett. **109**, 226405 (2012).

[39] W. Kohn and L. J. Sham, Phys. Rev. **140**, A1133 (1965).

[40] J. P. Perdew, K. Burke, and M. Ernzerhof, Phys. Rev. Lett. **77**, 3865 (1996).

[41] M. Srebro and J. Autschbach, J. Phys. Chem. Lett. **3**, 576 (2012).

[42] D. A. Egger, S. Weissman, S. Refaely-Abramson, S. Sharifzadeh, M. Dauth, R. Baer, S. Kümmel, J. B. Neaton, E. Zojer, and L. Kronik, J. Chem. Theo. Comput. **10**, 1934 (2014).

[43] M. A. Rohrdanz, K. M. Martins, and J. M. Herbert, J. Chem. Phys. **130**, 054112 (2009).

[44] E. Livshits and R. Baer, Phys. Chem. Chem. Phys. **9**, 2932 (2009).

[45] J.-D. Chai and M. Head-Gordon, Phys. Chem. Chem. Phys. **10**, 6615 (2008).

[46] J. P. Perdew, R. G. Parr, M. Levy, and J. L. Balduz, Phys. Rev. Lett. **49**, 1691 (1982).

[47] C.-O. Almbladh and U. von Barth, Phys. Rev. B **31**, 3231 (1985).

[48] J. P. Perdew and M. Levy, Phys. Rev. B **56**, 16021 (1997).

[49] M. Levy, J. P. Perdew, and V. Sahni, Phys. Rev. A **30**, 2745 (1984).

[50] T. Stein, L. Kronik, and R. Baer, J. Chem. Phys. **131**, 244119 (2009).

[51] T. Stein, J. Autschbach, N. Govind, L. Kronik, and R. Baer, J. Phys. Chem. Lett. **3**, 3740 (2012).

[52] J. Autschbach and M. Srebro, Acc. Chem. Res. **47**, 2592 (2014).

[53] T. Körzdörfer and J.-L. Brédas, Acc. Chem. Res. **47**, 3284 (2014).

[54] I. Tamblyn, S. Refaely-Abramson, J. B. Neaton, and L. Kronik, J. Phys. Chem. Lett. **5**, 2734 (2014).

[55] Y. Shao, Z. Gan, E. Epifanovsky, A. T. Gilbert, M. Wormit, J. Kussmann, A. W. Lange, A. Behn, J. Deng, X. Feng, et al., Mol. Phys. **113**, 184 (2015).

[56] J. Ihm, A. Zunger, and M. L. Cohen, J. Phys. C: Solid State Phys. **12**, 4409 (1979).

[57] N. Troullier and J. L. Martins, Phys. Rev. B **43**, 1993 (1991).

[58] *http://www.abinit.org/*.

[59] A. Tkatchenko, R. A. DiStasio, R. Car, and M. Scheffler, Phys. Rev. Lett. **108**, 236402 (2012).

[60] J. Deslippe, G. Samsonidze, D. A. Strubbeda, M. Jain, M. L. Cohen, and S. G. Louie, ChemPhysChem **183**, 1269 (2012).

[61] M. Rohlfing and S. G. Louie, Phys. Rev. B **62**, 4927 (2000).

[62] N. Sato, K. Seki, and H. Inokuchi, J. Chem. Soc., Faraday Trans. 2 **77**, 1621 (1981).

[63] J. B. Neaton, M. S. Hybertsen, and S. G. Louie, Phys. Rev. Lett. **97**, 216405 (2006).

[64] Z.-h. Yang, F. Sottile, and C. A. Ullrich, Phys. Rev. B **92**, 035202 (2015).

[65] T. Shimazaki and T. Nakajima, J. Chem. Phys. **142**, 074109 (2015).

[66] T. Shimazaki and T. Nakajima, Phys. Chem. Chem. Phys. **18**, 27554 (2016).

[67] J. H. Skone, M. Govoni, and G. Galli, Phys. Rev. B **93**, 235106 (2016).

[68] N. P. Brawand, M. Vörös, M. Govoni, and G. Galli, Phys. Rev. X **6**, 041002 (2016).

[69] H. Phillips, Z. Zheng, E. Geva, and B. D. Dunietz, Org. Electronics **15**, 1509 (2014), ISSN 1566-1199.

[70] H. Sun, S. Ryno, C. Zhong, M. K. Ravva, Z. Sun, T. Körzdorfer, and J.-L. Brédas, J. Chem. Theo. Comput. **12**, 2906 (2016).

[71] S. G. Warren, Appl. Optics **25**, 2560 (1986).

[72] K. Dressler and O. Schnepp, J. Chem. Phys. **33**, 270 (1960).

[73] W. R. Donaldson and C. L. Tang, Appl. Phys. Lett. **44**, 25 (1984).

[74] L. Landt, K. Klünder, J. E. Dahl, R. M. K. Carlson, T. Möller, and C. Bostedt, Phys. Rev. Lett. **103**, 047402 (2009).

[75] J. P. Doering, J. Chem. Phys. **67**, 4065 (1977).

[76] E. A. Silinsh, *Organic Molecular Crystals* (Springer-Verlag, Berlin, 1980).

[77] M. Pope and C. E. Swenberg, *Electronic Processes in Organic Crystals and Polymers* (Oxford University Press, New York, 1999).

[78] T. P. Lewis and H. R. Ragin, J. Am. Chem. Soc. **94**, 5566 (1972).

[79] T. J. Aartsma and D. A. Wiersma, Chem. Phys **1**, 211 (1973).

[80] W. A. Eaton and T. P. Lewis, J. Am. Chem. Soc. **53**, 2164 (1970).

[81] T. P. Lewis and W. A. Eaton, J. Am. Chem. Soc. **93**, 2054 (1971).

[82] C. Faber, C. Attaccalite, V. Olevano, E. Runge, and X. Blase, Phys. Rev. B **83**, 115123 (2011).

[83] N. Marom, X. Ren, J. E. Moussa, J. R. Chelikowsky, and L. Kronik, Phys. Rev. B **84**, 195143 (2011).

[84] N. Marom, F. Caruso, X. Ren, O. T. Hofmann, T. Körzdörfer, J. R. Chelikowsky, A. Rubio, M. Scheffler, and P. Rinke, Phys. Rev. B **86**, 245127 (2012).

[85] X. Blase, C. Attaccalite, and V. Olevano, Phys. Rev. B **83** (2011).

[86] T. Rangel, K. Berland, S. Sharifzadeh, F. Brown-

Altvater, K. Lee, P. Hyldgaard, L. Kronik, and J. B. Neaton, Phys. Rev. B **93**, 115206 (2016).

TABLE II: Energy of the lowest singlet excitation and position of lowest-lying main optical absorption peak, calculated using TD-OT-SRSH and the G_0W_0-BSE for the X23 set of molecular solids. Experimental values, where available, are provided for comparison. All energies are in eV.

Molecular Solid	First Excited State (S_1) Energy				Optical Peak Position		
	TD-LDA	TD-OT-SRSH	G_0W_0-BSE	Expt.	TD-LDA	TD-OT-SRSH	G_0W_0-BSE
Carbon dioxide	6.4	8.9	8.3	8.9[71]	7.2	10.7	10.8
Ammonia	4.3	6.7	6.6	6.6[72]	4.6	7.1	7.1
Cyanamide	4.6	6.0	5.4	-	5.6	7.3	7.1
Formamide	4.5	5.9	5.4	-	5.3	7.5	7.5
Urea	4.8	7.1	6.5	6.2[73]	6.4	7.4	7.1
Ethyl carbamate	5.6	7.3	6.5	-	7.2	7.7	7.5
Acetic acid	5.1	5.8	5.6	-	5.5	8.2	8.3
Oxalic acid (α)	3.2	4.7	4.4	-	3.7	6.0	6.3
Oxalic acid (β)	3.4	4.8	4.5	-	3.7	6.1	6.3
Succinic acid	5.0	6.2	5.7	-	5.4	8.7	8.6
Adamantane	4.8	6.8	6.8	6.5[74]	6.8	8.2	8.5
Hexamine	4.7	6.0	6.2	-	5.4	6.6	6.9
Trioxane	5.8	8.2	7.9	-	6.3	8.3	8.1
1,4-Cyclohexane-di-one	3.2	4.5	3.9	-	3.9	6.2	6.3
Benzene	4.3	5.4	4.9	4.7[75]	4.9	6.3	6.5
Naphthalene	3.1	4.2	4.1	3.9[76]	3.3	4.7	4.4
Anthracene	2.0	2.9	3.2	3.1[77]	2.1	3.0	3.2
Pyrazine	2.7	4.0	3.5	3.8[78]	3.0	4.0	3.5
Triazine	2.8	4.4	3.9	3.7[79]	3.4	4.6	4.2
Pyrazole	4.8	6.7	6.5	-	5.5	6.8	6.5
Imidazole	4.5	6.3	6.3	-	5.0	6.4	6.3
Uracil	3.4	4.6	4.9	4.5[80]	3.8	5.1	4.9
Cytosine	3.4	4.7	4.9	4.4[81]	3.8	5.0	4.9